Z. Phys. C - Particles and Fields 18, 289-299 (1983)

Zeitschrift für Physik C Particles and Fields

Observation of Light Below Cerenkov Threshold in a 1.5 Meter Long Integrating Cerenkov Counter

A. Bodek, W. Marsh[1]
University of Rochester, Rochester, NY 14627, USA

M.V. Purohit
California Institute of Technology, Pasadena, CA 91125, USA

P.S. Auchincloss, R. Blair, M.A. Ruiz,
F.J. Sciulli, M.H. Shaevitz
Columbia University, New York, NY 10027, USA

H.E. Fisk, T. Kondo[2], S. Pordes,
P.A. Rapidis, D.D. Yovanovitch
Fermilab, Batavia, IL 60510, USA

M. Abolins, R. Brock, D. Owen
Michigan State University, East Lansing, MI 48824, USA

K.A. Jenkins, O. Fackler
Rockefeller University, New York, NY 10021, USA

Received 28 March 1983

Abstract. We have observed Cerenkov light, well below threshold, in an integrating Cerenkov counter used to determine particle composition of the secondary hadron beam, which is the source of Fermilab narrow-band neutrinos. The phenomenon can be understood in terms of diffraction effects in a finite length counter caused by radiation emitted by particles traversing the counter even when it is evacuated. At zero pressure, the light can be considered as transition radiation produced when particles enter and leave the counter. A standard Cerenkov diffraction formula describes both the normal Cerenkov radiation and the light emitted below Cerenkov threshold.

1. Introduction

The emission of Cerenkov light [1] by a charged particle moving with velocity βc in a medium of refractive index n is usually treated as a 'shock-wave' phenomenon, yielding the condition that $\cos\theta_c = 1/n\beta$ where θ_c is the angle between the direction of particle motion and the emitted light. An alternative derivation [2] of this Cerenkov condition simply invokes conservation of energy and momentum in the process particle→particle + photon and yields the expression $\cos\theta_c = \frac{1}{n\beta}\left(1+\frac{\hbar\omega}{2E}(n^2-1)\right)$ where E is the energy of the radiating particle, and ω the frequency of the radiation. For $\hbar\omega \ll E$, as is the case for very high energy beams, this is the same as the result obtained using the shock-wave treatment. In both treatments, the Cerenkov light is emitted at a unique angle and only when the condition $n\beta > 1$ is satisfied.

A more complete treatment of Cerenkov light emitted in radiators of finite length [3-5] shows that the radiation is not produced at a unique angle but is in fact produced with a diffraction-like angular intensity distribution. This distribution has a peak at the nominal Cerenkov angle, and a spacing between lobes given by $\Delta\theta = \lambda/L\sin\theta_c$ where λ is the wavelength of the light, L the length of the radiator and θ_c the Cerenkov angle. It is known that these diffraction effects can limit the ability of Cerenkov counters to resolve different particles [5, 6]. Usually, however, gas-filled counters designed to identify individual particles at high energies operate at Cerenkov angles of 5 to 10 milliradians and are made tens of meters long in order to obtain sufficient light (the total light output being proportional to $L\sin^2\theta_c$). Cerenkov counters used simply to determine the composition of secondary beams [7, 8], that is the relative fractions of pions, kaons and protons, can be made to operate in an integrating mode since they do not attempt to identify individual particles and are typically required to operate at very high intensity. Such counters can be made short and operate at small (<2 milliradians) Cerenkov angles, since it is not necessary that each beam particle produce several photons. However, it is important to realize that diffraction effects in such short counters can be important, and must be understood in order to determine the beam composition correctly.

1 Present address: Fermilab Batavia, IL 60510, USA
2 Present address: National Laboratory for High Energy Physics (KEK Oho-Machi, Tsukuba-Gun, Ibaraki-Ken, 305 Japan

The broadening of the Cerenkov cone in a finite length counter implies that a particle with a given velocity, βc, will emit light at angles both smaller and larger than the nominal Cerenkov angle. Although it is implicit in the diffraction formula, it is not generally realized that the same effect implies that light will be emitted below Cerenkov threshold [4, 5], and that light can be observed even when the counter is evacuated. We will show that the remnant light at zero gas pressure can be attributed to transition radiation generated when particles enter and leave the counter. For any finite pressure, the identification of this light as transition radiation rather than Cerenkov radiation is in a sense a matter of nomenclature because the light is a coherent superposition of both effects.

In this note we report on the observation of such light as an aspect of the operation of Cerenkov counters subject to significant diffraction effects. Such counters are presently used for the determination of the particle composition of secondary beams for neutrino experiments at CERN [7] and at Fermilab [8]. The understanding of the properties of such counters is important since incorrect particle fractions can be obtained if the diffraction tails are mistakenly interpreted as backgrounds.

2. The Experimental Set-up and Technique

We shall discuss data obtained with two different Cerenkov counters used to determine the particle composition of the secondary beam, which acts as the source for the narrow-band neutrino beam at Fermilab [9]. Counter A was used initially in Fermilab experiment E356 [10] and was modified for later use in experiment E616 [8]. Counter B was used in experiments E594 and E701. The radiator in counter A was 1.9 m long, while that in counter B was 1.5 m long. Cerenkov light was viewed at a fixed angle, typically 1 milliradian, for counter A. For counter B, data were taken at angles of 1 and 2 mr.

The optical systems of counters A and B are shown in Figs. 1 and 2, respectively (all the mirrors had front-coated surfaces). In Counter A the Cerenkov light was focussed by mirror 1 onto an annular iris after reflecting from mirrors 2 and 3. Mirror 4 directed the light through a lens which focussed the light onto a photo-multiplier. The Ce-

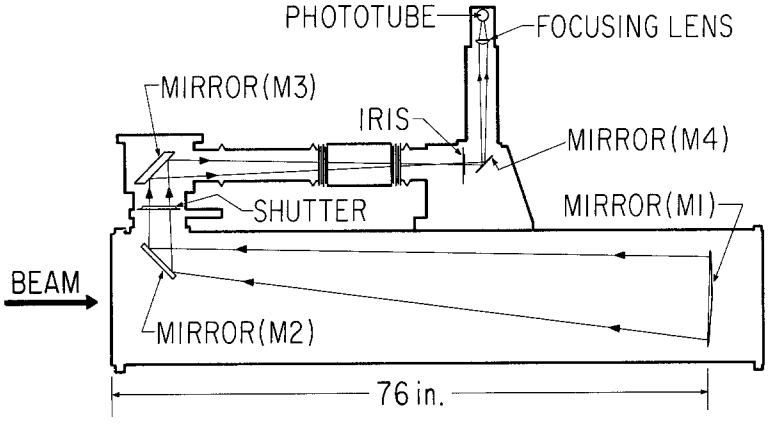

Fig. 1. Cerenkov Counter A (used in Fermilab experiments E356 and E616)

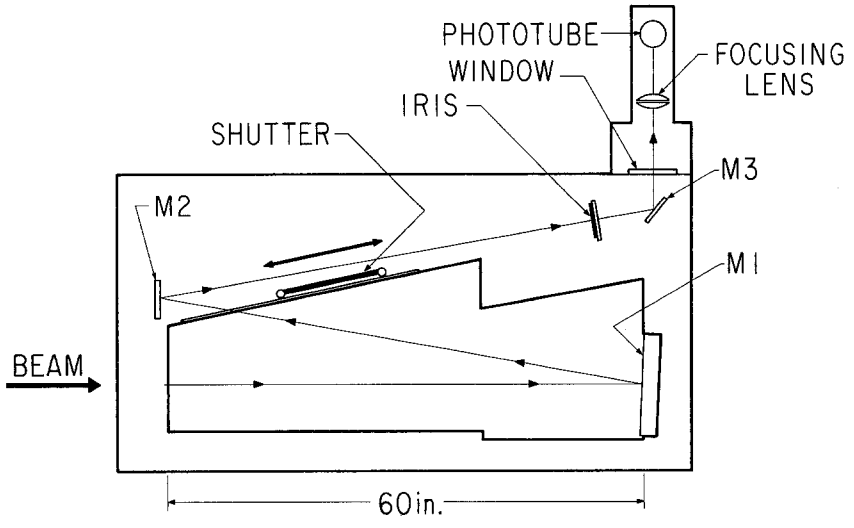

Fig. 2. Cerenkov Counter B (used in Fermilab experiments E594 and E701)

renkov light emitted at an angle θ was focussed to a circle at the location of the iris of radius $f(\tan\theta)$ where f is the focal length of mirror 1. The 1 mr annular iris blocked all light except rays for Cerenkov angles between 0.7 mr and 1.0 mr, (corresponding to $\langle\theta^2\rangle = 0.774\times10^{-6}$). The shutter between mirrors 2 and 3 could be closed remotely. The closed shutter measurements were used to determine the level of background light not originating from the main body of the Cerenkov counter. In counter B the light was focussed onto the annular iris after reflecting from mirrors 1 and 2. The shutter for this counter was located between mirror 1 and mirror 2. Both counters had an additional shutter around the photo-multiplier to help identify background due to particles producing Cerenkov light in the glass of the phototube itself. Counter B was constructed with fewer mirrors in order to reduce the number of reflecting surfaces that could accumulate dust. Note that in both counters, the beam passed through the primary mirror (Mirror 1) which defined the downstream end of the radiator region.

The principles of the experimental technique can be illustrated by considering how an ideal Cerenkov counter with no diffraction effects could be used to determine the particle composition of a perfectly parallel beam of unique momentum p. The number of photons of wavelength λ emitted by a particle of velocity βc traversing a long ($L \gg \lambda/(\sin\theta_c)$) gas filled counter is given by [3]

$$\frac{dN}{d\lambda} = \frac{2\pi\alpha}{\lambda^2} L \sin^2\theta_c \tag{1}$$

where α is the fine structure constant. Light is emitted only at the Cerenkov angle θ_c which is given by

$$\cos\theta_c = \frac{1}{\beta n} \tag{2}$$

where n is the index of refraction of the gas. For a photo-multiplier tube with a typical quantum efficiency in the visible spectrum, the number of photoelectrons is given by [6, 11]

$$N_{\mathrm{pe}} = BL\sin^2\theta_c \tag{3}$$

where $B = 50$ to $60\,\mathrm{cm}^{-1}$ (for a glass phototube window) or $B = 100$ to $150\,\mathrm{cm}^{-1}$ (for a quartz phototube window). For a 1 meter long counter, operating at a 1 mr Cerenkov angle, the above equation yields 5×10^{-3} photoelectrons per particle. This illustrates that for such a counter the light intensity must be integrated over a large number of particles.

The pressure dependence of the index of refraction n for helium gas is given by the expression $n = 1 + kP_r$. Here P_r is the pressure and k is a constant which is proportional to $1/T$, where T is the absolute temperature. At room temperature, the average value of k for Helium gas is 4.308×10^{-8} $(\mathrm{Hgmm})^{-1}$, averaged over wavelengths ($\langle\lambda\rangle \simeq 4000$ Å) in the optical region.

For small Cerenkov angles, and β close to 1.0, (2) can be rewritten as

$$\theta_c^2 = 2kP_r - \frac{m^2}{p^2} \tag{4}$$

where m is the rest mass of the incoming particle. For a monoenergetic parallel beam traversing an ideal counter, with an annular iris before the phototube, accepting light at angles between θ_A and θ_B, light will be detected only for pressures between P_A and P_B where

$$P_A = \frac{1}{2k}(\theta_A^2 + m^2/p^2)$$
$$P_B = \frac{1}{2k}(\theta_B^2 + m^2/p^2). \tag{5}$$

The light intensity detected will be proportional to $\sin^2\theta$, for θ between θ_A and θ_B, and to the number of particles of mass m. If the beam contains several particle types, all of the same momentum but of different masses, e.g. positrons, muons, pions, kaons and protons, then there will be no light observed through the iris as the pressure is varied, except for pressures in bands which correspond to the regions between P_A and P_B for each particle type. The light intensity versus pressure is shown in Fig. 3 for this ideal case. Since the amount of Cerenkov light emitted by a particle only depends on θ_c and the iris accepts only a well defined angular interval, the integral of the light intensity in any given $(P_A - P_B)$ band is proportional to the number of positrons, muons, pions, kaons or protons in the beam. Such a pressure curve can therefore be used to determine, on a statistical basis, the fractional particle composition of any secondary beam.

The Cerenkov curve in Fig. 3 illustrates (for an ideal counter) the principle of determining particle fractions through the integrating technique. In practice, the pressure curve for each particle type is broadened by several effects, including the angular divergence of the beam, the finite momentum spread of the beam, the variations of the index of refraction with wavelength (optical dispersion), any optical aberrations in the counter, as well as by Cerenkov diffraction [12]. For our beam, the effective rms angular divergence is 0.14 mr and the effective momentum spread is 10%. The effective angular dispersion is in general smaller than the true dispersion, because part of the angular dispersion broadening can be compensated for by moving the iris from the focal point of the mirror (i.e. a source at infinity) to

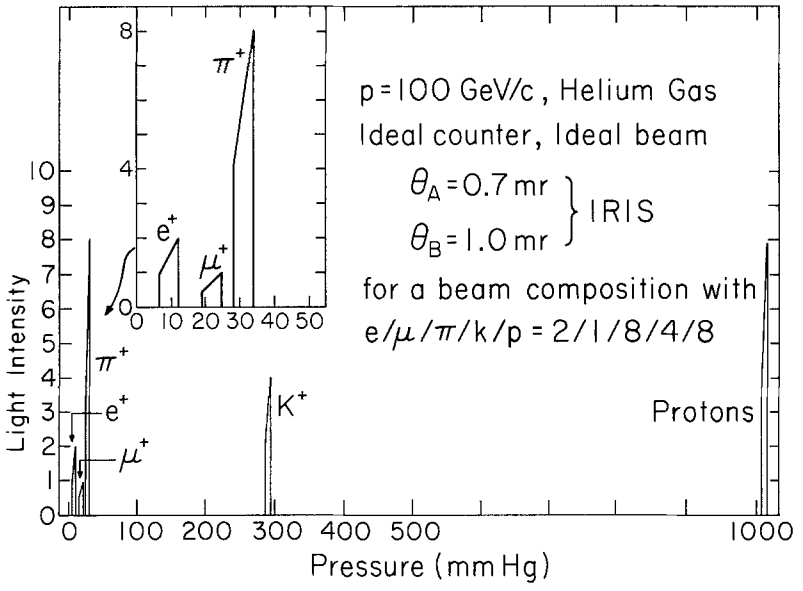

Fig. 3. Cerenkov pressure curve for a 200 GeV ideal beam and counter

the location of the focus for rays originating from the production target. The above beam-related dispersions produce a broadening of the angle of the Cerenkov cone, or, equivalently, smear the peaks in the Cerenkov pressure curves. For a 1 mrad iris, the broadening due to angular dispersion of the beam is given by

$$\Delta\theta_{\text{rms}} = 0.14\,\text{mrad}$$
$$(\Delta P_r) = \frac{\theta(\Delta\theta)}{k} = 2.9\,\text{mmHg}. \tag{6}$$

For a 200 GeV secondary beam, the broadening due to the 10% momentum bite is given (for pions, kaons and protons) by

$$\Delta\theta_{\text{rms}} = \frac{(\Delta p/p)}{\theta}\left(\frac{m^2}{p^2}\right)$$
$$= 0.06\,\text{mr}\,(\pi),\ 0.7\,\text{mr}\,(K),\ 2.5\,\text{mr}\,(p)$$
$$(\Delta P_r) = \frac{(\Delta p/p)}{k}\left(\frac{m^2}{p^2}\right) \tag{7}$$
$$= 1.1\,\text{mmHg}\,(\pi),\ 14\,\text{mmHg}\,(K),\ 50\,\text{mmHg}\,(p).$$

The variation of the index of refraction with wavelength leads to optical dispersion broadening. For Helium gas at atmospheric pressure and a temperature of 20° C the values of $n-1$ are [13] 33.27, 32.90 and 32.67 (in units of 10^{-6}) for wavelengths of 2800 Å, 3500 Å and 4400 Å, respectively. The variation of $n-1$ for $3500 < \lambda < 4500$ Å is $\pm 0.12 \times 10^{-6}$. This variation, weighted by the phototube spectral response, leads to the following dispersion broadening (for $\theta = 1$ mr)

$$\Delta\theta)_{\text{rms}} = \frac{\Delta n/n}{\tan\theta} = 0.13\,\text{mrad}$$
$$\Delta P_r = \left(\frac{\Delta n}{n-1}\right) P_r = (0.35\%)\,P_r. \tag{8}$$

The dispersion broadening yields $\Delta P_r = 0.05\,\text{mmH}_g$, $0.3\,\text{mmH}_g$ and $0.9\,\text{mmH}_g$ for 200 GeV pion, kaons and protons, respectively. In principle, these negligible optical dispersion effects can be completely eliminated if a narrow band optical filter is inserted in front of the phototube. The temperature of our Cerenkov radiator was monitored, so small variations in $n-1$ due to temperature changes can be corrected for. For example, temperature fluctuations of order 1 degree centrigrade $\left(\text{i.e. } \frac{\Delta n}{n} \approx 1/300\right)$ lead to a broadening which is similar to that due to dispersion (8). The broadening from optical imperfections and astigmatism due to off-axis optics are smaller than those due to diffraction effects discussed in the following section.

3. Diffraction Broadening

The number of photons per unit wavelength in a counter of finite length L is given by [3, 4]

$$\frac{d^2N}{d\lambda\, d\cos\theta} = \frac{2\pi\alpha}{\lambda}\left(\frac{L}{\lambda}\right)^2\left[\frac{\sin x}{x}\right]^2 \sin^2\theta \tag{9}$$

where in the equation above,

$$x(\theta) = \pi\frac{L}{\lambda}\left[\frac{1}{n\beta} - \cos\theta\right]. \tag{10}$$

For a gas Cerenkov counter operating at small angles and β close to 1 $x(\theta)$ can be rewritten as

$$x(\theta)=\frac{\pi L}{2\lambda}[1-\beta^2+\theta^2-2kP_r]$$
$$=\frac{\pi L}{2\lambda}\left[\frac{1}{\gamma^2}+\theta^2-2kP_r\right]$$
$$=\frac{\pi L}{2\lambda}\left[\frac{m^2}{p^2}+\theta^2-2kP_r\right]. \quad (11)$$

In the limit of having a very long counter ($L/\lambda\to\infty$), $\frac{\sin x}{x}$ becomes a δ-function and (9) becomes

$$\frac{d^2N}{d\lambda\, d\cos\theta}=\frac{2\pi^2\alpha}{\lambda}\delta(x)\left(\frac{L}{\lambda}\right)^2\sin^2\theta \quad (12)$$

which reduces to (1) when the δ function is integrated over all angles.

By setting $x=\pi$ in (10) (i.e. the first diffraction minimum) we see that $\Delta\theta_{\mathrm{DIFF}}$, the separation between the peak and the first diffraction minimum, is given by $\Delta\theta_{\mathrm{DIFF}}=\lambda/L\sin\theta=0.21$ mr. For $\theta=1$ mr, $L=1.9$ m, and λ of 4,000 Å, this $\Delta\theta_{\mathrm{DIFF}}$ corresponds to a pressure broadening of

$$(\Delta P_r)_{\mathrm{DIFF}}=\frac{\theta(\Delta\theta_{\mathrm{DIFF}})}{k}=5\,\mathrm{mmHg}. \quad (13)$$

Comparison of the various causes of broadening in a 1.9 m long Cerenkov counter shows that, at our energies, the broadening due to diffraction effects is the dominant source of broadening of the pressure curves for low mass particles such as electrons, muons and pions. For higher mass particles, such as kaons and protons, the momentum spread is more important if Δp is as large as $\pm 10\%$.

Diffraction broadening differs from other broadening effects because it results in radiation below Cerenkov threshold [4, 5]. The angular divergence of the beam, for example, can only broaden the angle of the Cerenkov cone and therefore there will be no light if the pressure is below the nominal Cerenkov threshold ($P_{\mathrm{threshold}}=m^2/2kp^2$). The diffraction formula (9), (11) however, predicts some radiation even at zero pressure (i.e., below threshold). This point is discussed in the following section.

4. Cerenkov Light and Transition Radiation

In the derivation of the Cerenkov diffraction formula, the boundary condition was imposed that no light is observed from regions outside the counter.

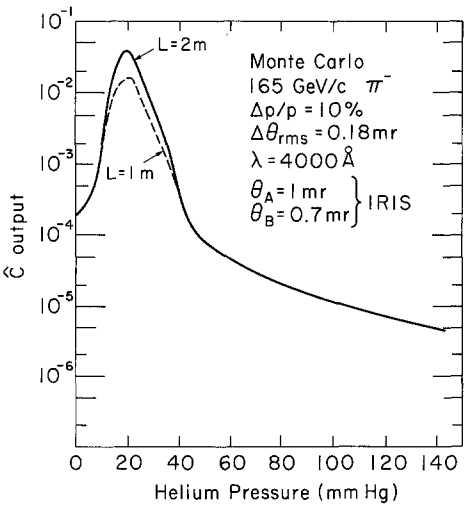

Fig. 4. Monte Carlo Cerenkov pressure curve for a 1 mr iris and a 165 GeV pion beam for a counter of $L=1$ m and $L=2$ m. Note that the low and high pressure tails due to diffraction effects are independent of the length of the counter. The light intensity at the peak is proportional to the length of the counter

This is equivalent to saying that for optical frequencies the dielectric constant (ε) of the counter windows is infinite. (That is, the value of $n-1$ of the windows is much larger than θ^2 or $1/\gamma^2$.) The transition radiation emitted in the process of the particle entering and leaving the counter is therefore an integral part of the formula. We will show that, for our data, (9) yields the correct level of transition radiation in the counter.

If we investigate the prediction of (9) and (11) in the region far from the nominal Cerenkov maximum (i.e. $x\neq 0$) (9) and (11) can be rewritten in the form (for small angles)

$$\frac{d^2N}{d\lambda\cos\theta}\approx\frac{8\alpha}{\pi\lambda}\frac{\theta^2\sin^2 x}{(1-\beta^2+\theta^2-2kP_r)^2}. \quad (14)$$

Note that for $|x|\gg 0$ the average value of $\sin^2 x$ is equal to 0.5 and (14) shows that the counter response at pressures away from the region of the Cerenkov maximum is independent of the length of the counter. Figure 4 shows the direct calculation of (9) for counters of length $L=1$ m and $L=2$ m, for a 1 mr iris, for λ in the visible region. The curve, calculated for a 165 GeV pion beam, shows that, while the response in the region of the peak changes by a factor of 2 for a counter with twice the length, the response on the high and low pressure tails is independent of the counter length. In order to illustrate the relationship between (14) and transition radiation, we let $L\to\infty$ (i.e. $\langle\sin^2 x\rangle=\frac{1}{2}$) and set the pressure to zero (i.e. vacuum). At zero pressure the expression yields

$$\frac{d^2N}{d\lambda\, d\cos\theta}=\frac{4\alpha}{\pi\lambda}\frac{\theta^2}{[1-\beta^2+\theta^2]^2}. \tag{15}$$

Some physical insight into the origin of this radiation may be obtained by noting that this form is very similar to the formula for the radiation emitted when a particle crosses a boundary between two media (that is, transition radiation) [14]. Equation (15) is related to the formula for transition radiation [15]

$$\frac{d^2N}{d\lambda\, d\cos\theta}=\frac{2\alpha}{\pi\lambda}\frac{\sin^2\theta\cos^2\theta}{(1-\beta^2\cos^2\theta)^2}\cdot\left|\frac{(\varepsilon-1)(1-\beta^2\mp\beta(\varepsilon-\sin^2\theta)^{\frac{1}{2}})}{(\varepsilon\cos\theta+(\varepsilon-\sin^2\theta)^{\frac{1}{2}})(1\mp\beta(\varepsilon-\sin^2\theta)^{\frac{1}{2}})}\right|^2 \tag{16}$$

derived for radiation emitted at the boundary between vacuum and a single plate of dielectric constant $\varepsilon=a(\lambda)+ib(\lambda)$. The minus sign in (16) refers to radiation in the forward direction, or into the vacuum (i.e. a plate-vacuum transition), the positive sign refers to radiation in the backward direction (i.e. a vacuum-plate transition). For optical frequencies, $|\varepsilon|$ is $\gg 1$, and for $\beta\to 1$ and small θ, (16) reduces to (17a), and (17b) for forward, and backward transition radiation, respectively.

$$\frac{d^2N}{d\lambda\, d\cos\theta}=\frac{2\alpha}{\pi\lambda}\frac{\theta^2}{(1-\beta^2+\theta^2)^2}, \tag{17a}$$

$$\frac{d^2N}{d\lambda\, d\cos\theta}=\frac{2\alpha}{\pi\lambda}\frac{\theta'^2}{(1-\beta^2+\theta'^2)^2}\left|\frac{\sqrt{\varepsilon}-1}{\sqrt{\varepsilon}+1}\right|^2. \tag{17b}$$

Where θ' in (17b) is $\pi-\theta$.

Note that the ratio of (17b) to (17a) is just the reflectivity of the mirror which in the optical range is very close to 1. Both the forward Cerenkov radiation and the transition light from the upstream window must reflect from the mirror before reaching the phototube. Therefore, the intensity reaching the phototube from the forward transition light will be the same as from the backward radiation from the mirror. Equation (17a) is precisely a factor of 2 smaller than (15), as expected because of the two counter interfaces (the upstream window and the downstream mirror). This factor of 2 is correct in the limit $L\to\infty$ because in that case the light from the two interfaces cannot interfere. In a finite length counter, the contributions of the two interfaces interfere with each other (see Appendix B). The fact that the downstream interface (i.e. the mirror) is tilted by about 5° does not change our conclusion because the direction of the backward transition radiation is along *the mirror reflection* [16] of the direction of the incident particle (see Appendix B). The diffraction formula (which assumes $\varepsilon=\infty$ for the interfaces) should work very well in the region of the Cerenkov maximum; at zero pressure we expect the expression to represent the radiation in the counter within the accuracy of our measurement, i.e. about 10%.

Experimental observation of transition radiation at optical frequencies was reported [17] in the late 1950's. Previous observations [18] of radiation below threshold for electrons in water have also been attributed to diffraction effects. In the 1960's several experiments [19] have observed transition radiation in the optical frequencies in agreement with theoretical calculations. The fact that backward optical transition radiation from an inclined plane is emitted along the mirror reflection of the incident particle direction has been experimentally confirmed by more recent experiment [20] with electrons. These experiments have also observed interference between transition radiation emitted by two foils.

In the following sections we will present experimental evidence that the diffraction formula describes the radiation observed in the counter at all pressures. In the Cerenkov cone region it describes the diffraction broadening and for the case of an evacuated counter it describes the amplitude and angular distribution of the transition radiation emitted when the particle enters and leaves the counter.

5. Data with 200 GeV Monochromatic Protons: The Region of the Diffraction Peak

The response of each Cerenkov counter to a truly monoenergetic beam was obtained by exposing each to a 200 GeV extracted proton beam (such a beam has a momentum spread of $\Delta p/p$ less than 10^{-4}). To match the condition under which the secondary beam is studied, the beam intensity was varied between 10^{10} and 10^{11} particles delivered in a 3 ms pulse. The angular divergence of this beam ($\Delta\theta\leqq 0.1$ mr) was smaller than the typical angular divergence of secondary beams. The Cerenkov light was viewed using an annular iris which accepted light between 0.7 and 1.0 mr.

For such a monochromatic beam, the diffraction formula predicts that the response of the counter as a function of pressure is dominated by diffraction effects. The data as a function of pressure is shown in Fig. 5. The solid line is the prediction of a Monte Carlo calculation which includes effects due to the angular divergence of the beam, optical dispersion, and the detailed optics of the counter (i.e. the off-axis optics) as well as the basic diffraction formula. The agreement in the region of the peak is excellent

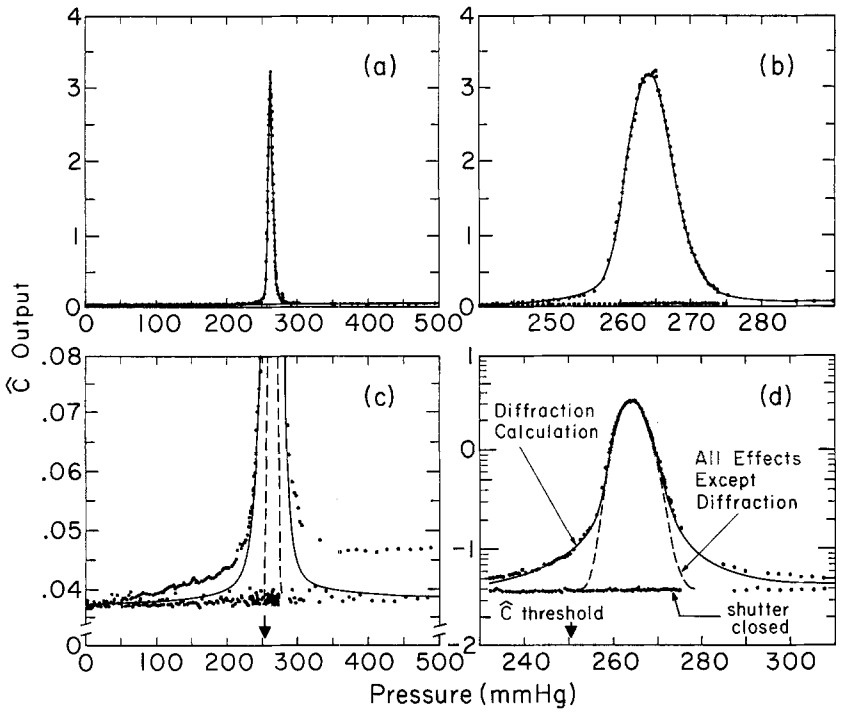

Fig. 5 a–d. Data and the diffraction formula prediction for monochromatic 200 GeV protons. Note that diffraction effects result in light below Cerenkov threshold for 200 GeV protons. The dashed line is the Monte Carlo without diffraction. Data were taken with counter *B* (experiments E594/E701)

over three orders of magnitude. The dashed line in Fig. 5 is the prediction of the Monte Carlo without diffraction, but including all other effects.

6. Backgrounds

Data were taken with the main shutter of the counter open and closed on alternate beam pulses every 12 s. The closed shutter data measure the background light level from sources outside the main body of the counter. We determined that the dominant source of this light comes from Cerenkov radiation produced by halo particles in the glass walls of the phototube and in the lenses of the optics system. The black surfaces on the inside of the counters were tested and found not to be optically active at any significant level. Both shutter-open and shutter-closed data are shown in Fig. 5. As can be seen, the level of the shutter-closed data is nearly constant, with very little dependence on the gas pressure. The level of the shutter-closed data has therefore been added to the Monte Carlo before comparison with the data. The agreement between our Monte Carlo prediction and the data, and especially the fact that part of the peak is in a region below the absolute Cerenkov-threshold pressure, is a confirmation of the validity of the diffraction formula. Again, note that the dashed line in Fig. 5 is a prediction of the Monte Carlo without diffraction, but including all other effects.

Far away from the diffraction peak there are additional tails in the data that are not predicted by the Monte Carlo calculation. These low level tails are due to other effects. The tail at high pressure has a contribution from scattering of light from dust particles on the mirror (at the level of 10^{-4} of the primary Cerenkov light). We observed that this tail decreased after the mirrors were cleaned. The tail at low pressure and some part of the high pressure tail have contributions from interactions of the beam in material upstream of the counter. Both low pressure and high pressure tails increased when additional material was introduced in front of the Crenkov counter. When the amount of material in front of the counter was increased by a factor of 5, only the tails far from the peak increased in amplitude, while the large diffraction tails near the peak remained unchanged.

Note that the prediction, based on the Cerenkov diffraction formula, shown in Fig. 5 indicates essentially no light for protons at very low pressures. In transition-radiation terms, this is because 200 GeV protons do not have large γ; in terms of the diffraction formula, this is because zero-pressure is some 50 diffraction minima from the peak. Light at zero-pressure is observed primarily from particles such as pions and electrons with large γ, as discussed in the next section.

7. Data with Pions, Kaons and Protons

Figure 6 shows typical (1 mr iris) Cerenkov pressure curves taken with secondary beams containing

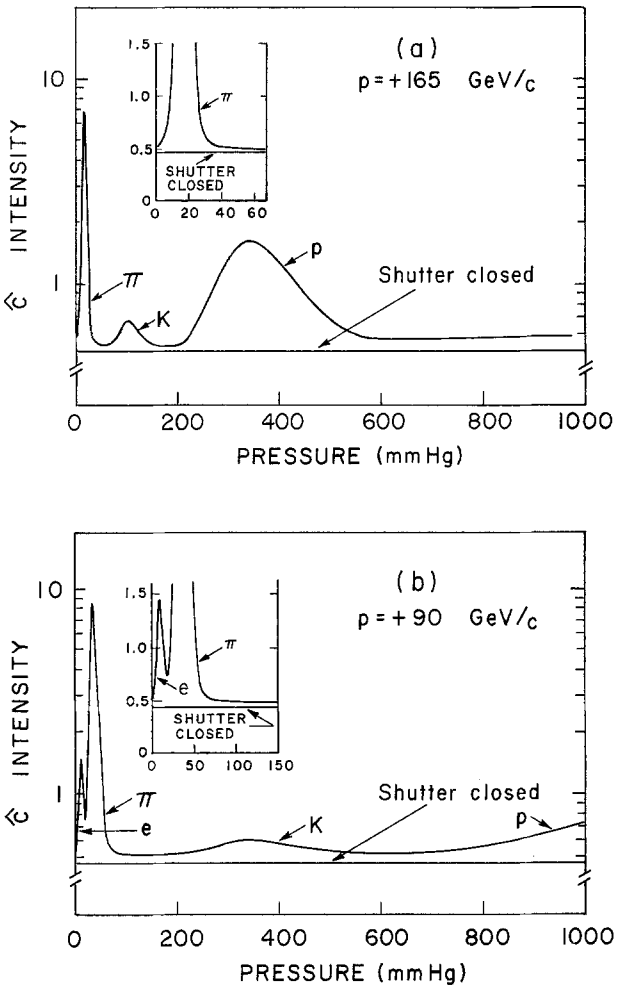

Fig. 6 a and b. Typical Cerenkov pressure curves taken with a 10% momentum bite secondary beam containing pions, kaons and protons

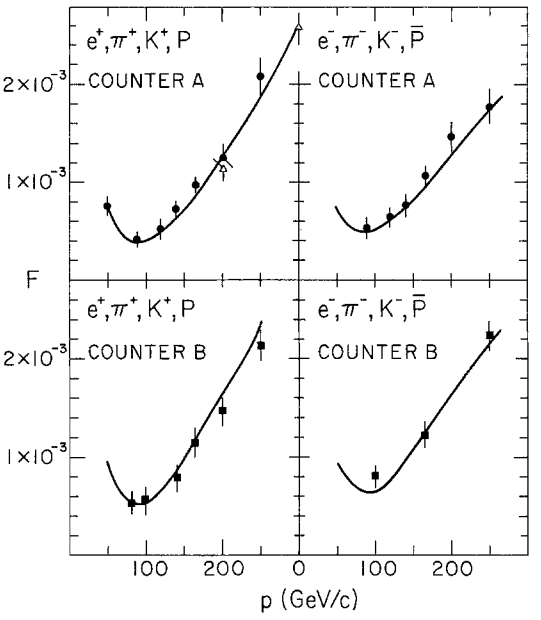

Fig. 7. Ratio of light at zero pressure to the integral of the light intensity at higher pressure over the electron and pion peak region. The curve is the prediction of the diffraction formula Monte Carlo (see Appendix A). (●) Data from experiment E616, (■) data from experiments E594/E701. (△) data from experiment E356

pions, kaon and protons. The secondary beams [8, 9] were produced by targeting 400 GeV protons on 26.7 cm, and 30.5 cm long BeO targets for the data taken with counters *A*, and *B*, respectively. The decays of pions and kaons yield narrow-band neutrino beams used by Fermilab neutrino experiments. The secondary hadron beam has the properties described previously in Sect. 2. Pions, kaons and protons are clearly resolved at all energies. Electrons can be resolved from pions only at the lower energies (below 120 GeV) but pions and muons cannot be separated. A calculation [8] of the electron fraction of the beam (which includes sources such as Dalitz decays and photon conversions) agrees with the measurements at lower energies and predicts a small electron contribution ($<3\%$) at the higher energies. As the curves indicate, there is a significant and reproducible amount of light in the counter even when the counter is evacuated to a pressure of 1 micron (shown as zero pressure). At this pressure all known particles at beam momentum are below Cerenkov threshold. As discussed in previous sections, this light can be identified with transition radiation, emitted as the particles enter and leave the counter. Figure 7 shows the measured ratio of the light intensity at zero pressure to the integral over pressure of the light intensity for pions and electrons. The solid curve, which is discussed in detail in Appendix A, is the prediction of the diffraction formula. The agreement is within the expected 10%.

8. The Angular Dependence of the Zero Pressure Light

We have investigated the possibility that the light at zero pressure originates from excitation in the upstream window (e.g. scintillation light). Such light would be isotropic and hence would not depend on the orientation of the counter with respect to the direction of the beam. At zero pressure, the transition radiation is peaked forward, so the the observed intensity should be strongly dependent on the angle between the counter and the beam. To study this we replaced the annular iris with a hole which accepted all light with $\theta \leqq 0.5$ mr. Figure 8 shows the intensity at zero pressure for $\theta \leqq 0.5$ mr as a function

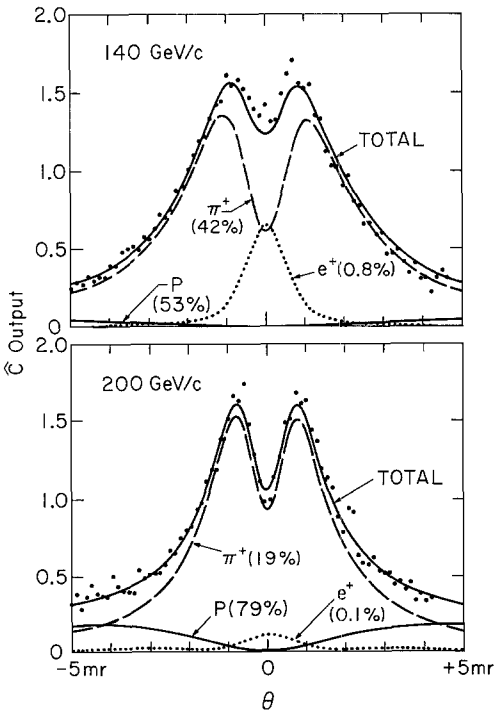

Fig. 8. The light intensity at zero pressure (for a 0.5 mr hole) as a function of the angle θ of the counter with respect to direction of the particle beam. These data indicate that the light is associated with the beam direction (e.g. transition radiation) and therefore cannot be uniform scintillation light from excitations in the wall. Also shown is the prediction of the diffraction formula Monte Carlo for 140 GeV (assuming 0.83% e^+, 42% π^+, 4.22% K^+ and 53.4% protons) and for 200 GeV (assuming 0.11% e^+, 18.9% π^+, 2.3% K^+ and 78.7% protons). Data were taken with Counter *B* (E594/E701)

of the angle between the axis of the Cerenkov counter and the incident beam. The solid curves (which are described in detail in Appendix A) are the predictions of the diffraction formula at zero pressure. The dramatic difference in the angular distribution of transition light produced by electrons as compared to heavier particles is due to the difference in the phase angle [x in (11)] in the interference term of the diffraction formula. The momentum dependence of the shapes of the curves in Fig. 8 is primarily due to the change in the particle composition of the beam. The curves also illustrate that at high energies (when the Cerenkov counter cannot resolve the electron peak) the angular distribution of the transition radiation can be used to determine the electron fraction of the beam.

We conclude that the diffraction formula for light in a finite length Cerenkov counter describes the radiation in the counter at all pressures including the case when the counter is fully evacuated. The non-zero result from the formula in the zero pressure limit is understood in terms of transition radiation.

Our data indicate that when integrating Cerenkov counters of short length are used in the determination of the composition of secondary beams, the tails due to diffraction must be included in the analysis of the pion, kaon and proton peaks. A Monte Carlo program which includes diffraction effects should be used to determine corrections that relate the relative areas to the fractional particle composition of the beam. In addition, our experience indicates that the analysis is simpler when integrating counters are tens of meters long, since this minimizes diffraction broadening.

Acknowledgements. We thank the management and staff of the Fermi National Accelerator Laboratory and especially the Neutrino Department, the Accelerator Division and the Physics Department for their support. We thank our collaborators in experiments E356, E616, E594 and E701 during which the Cerenkov data were taken and R. Walker who originally pointed out the importance of diffraction effects in our counter. This work was supported by the U.S. Department of Energy and the National Science Foundation.

Appendix A: Transition Light and Cerenkov Light

For a beam with a finite angular divergence and a finite momentum spread the integral over pressure of the Cerenkov intensity at a fixed angle is proportional to the total number of particles. The integral over pressure of (9) is

$$I_c=\frac{4\pi\alpha}{\lambda}\frac{L}{\lambda(2k)}\theta^2 d\cos\theta. \tag{A1}$$

At zero pressure, the total amount of transition light is proportional to the number of particles. The diffraction formula predicts transition light intensity at the level of

$$I_T=\frac{4\alpha}{\pi\lambda}\frac{2\sin^2\left\{\frac{\pi L}{2\lambda}[\theta^2+m^2/p^2]\right\}}{[\theta^2+m^2/p^2]^2}\theta^2 d\cos\theta. \tag{A2}$$

This formula is the same as the formula for the interference of transition radiation from two foils given by Wartski et al. [20]. The ratio of the zero pressure light to the integral over pressure is

$$f=\frac{I_T}{I_c}=\frac{(2k)\lambda}{\pi^2 L}\left[\frac{\sin^2\left(\frac{\pi L}{2\lambda}[\theta^2+m^2/p^2]\right)}{[\theta^2+m^2/p^2]^2}\right]. \tag{A3}$$

For helium gas ($2k=8.6\times10^{-8}$ $H_g$mm^{-1}), $L=1.9$ m, a 0.7/1.0 mr iris ($\langle\theta^2\rangle=0.8\times10^{-6}$) and $\lambda\cong4000$ Å, (A3) yields.

$$f \cong 3\times 10^{-3}\frac{2\sin^2\left\{9.3\left(1+\frac{m^2/p^2}{0.8\times 10^{-6}}\right)\right\}}{\left(1+\frac{m^2/p^2}{0.8\times 10^{-6}}\right)^2}. \quad (A4)$$

The interference term between the radiation emitted when the particle enters and the radiation emitted when the particle leaves the counter averages to approximately 0.5 when (A3) is integrated over all wavelengths in the visible region and over the finite momentum of the beam. In that case we obtain

$$f \cong \frac{3\times 10^{-3}}{\left(1+\frac{m^2/p^2}{0.8\times 10^{-6}}\right)^2}. \quad (A5)$$

For $p=200\,\text{GeV/c}$, the term m^2/p^2 is 6.5×10^{-12}, 0.49×10^{-6}, 6.1×10^{-6} and 22×10^{-6} for electrons, pions, kaons and protons respectively. Therefore, pions and electrons will be the dominant source of the zero pressure light. The relative contribution of electron to the zero pressure light is a function of the momentum p, and the electron fraction of the beam. At $p=50\,\text{GeV/c}$ the electron contribution dominates and for $p\geqq 90\,\text{GeV/c}$ the pion contribution dominates. The contribution of protons is small except at the highest momenta ($p\geqq 250\,\text{GeV/c}$) where the proton fraction of the beam is large.

We have calculated the quantity F, the ratio of the zero pressure light level to the integral over the electron and pion peaks (using (A3)).

$$F=\frac{\sum f_i R_i}{R_1+R_2} \quad (A6)$$

where f_1, f_2, f_3 and f_4 are from (A3) (averaged over λ in the visible region) for electrons, pions, kaons and protons, respectively and R_1, R_2, R_3, R_4 are the fractional composition of electrons, pions, kaons and protons in the secondary beam.

The comparison of the measured values of F and the calculated values are shown in Fig. 7. The calculated curves were obtained from a Monte Carlo calculation which did not incorporate any of the approximations used in (A4) and (A5).

In the study of the angular distribution of the zero pressure light the 0.7/1.0 mr iris was replaced with a 0.5 mr hole. For $L=1.9\,\text{m}$ and $\lambda\cong 4000\,\text{Å}$ (A2) yields

$$I_T=\frac{4\alpha}{\pi\lambda}\frac{2\sin^2[0.37\times 10^7(\theta^2+m^2/p^2)]}{[\theta^2+m^2/p^2]^2}\theta^2\, d\cos\theta. \quad (A7)$$

The situation for $\theta<0.5\,\text{mr}$ is different from the case of the 0.7/1.0 mr iris. At $\theta\simeq 1\,\text{mr}$, the phase angle in the numerator is large and $\langle\sin^2 x\rangle\cong 0.5$ when averaged over λ. On the other hand, close to $\theta=0$, the phase angle is small and does not average to 0.5. This phase angle will be different for the electron and pion components in the beam.

The values for the fractional particle composition used in the calculations of the curves for Figs. 7 and 8 were obtained from a preliminary analysis of the Cerenkov curves. Final particle fractions will be published in future communications. The electron fractions used were those calculated in [8].

The zero pressure intensity for $\theta<0.5\,\text{mr}$ is shown in Fig. 8 as a function of the angle of the axis of the Cerenkov counter with respect to the incident beam. The solid curve is the sum of the contributions from the electron, pion, kaon and proton components of the beam. The depth of the dip at $\theta=0$ in the sum of all components is very sensitive to the electron to pion ratio because the electron contribution peaks at $\theta=0$ and the pion contribution peaks at $\theta=\pm 1\,\text{mr}$. Thus the good agreement between the Monte Carlo calculation and the data at *all momenta* is not only an experimental confirmation of the diffraction formula but also a check of the electron fractions calculated in [8].

Appendix B: Transition Radiation from Inclined Surfaces

The downstream interface in the Cerenkov counter is the spherical mirror which focusses the light onto the iris. This mirror is inclined at about 5° with respect to the direction of the incident beam.

Transition radiation from particles incident on an inclined surface has been originally calculated by Pafomov [15]. Recent detailed calculations [16] indicate that the angular distribution of the forward transition radiation (e.g. metal-vacuum interface) is peaked around the direction of the incident particle even when the interface is at an angle. The backward transition radiation (e.g. vacuum metal interface) from an inclined surface concentrates close to the direction of the *mirror reflection* of incident particle velocity vector. Therefore, after reflecting from the mirror, the angular distribution of the forward transition radiation emitted as the particle enters the counter, will be very close to that of the backward transition radiation emitted from the mirror as the particle leaves the counter. This property of backward transition radiation is the explanation of the, previously unexplained, large difference [19] between the angular distribution of forward and backward transition radiation observed in 1960's for particles traversing metal foils at an angle of 60°. De-

tailed studies of forward and backward optical transition radiation have been done by Wartski [20].

The transition radiation from the interfaces can also include some Cerenkov radiation which is generated in the window material but not fully absorbed [21], as well as radiation from surface irregularities [22]. We expect these, and effects due to the finite dielectric constant of the windows, to be smaller than the uncertainties in our data ($\simeq 10\%$).

References

1. P.A. Cerenkov: Phys. Rev. **52**, 378 (1937)
2. V.L. Ginzburg: J. Phys. USSR, **2**, 441 (1940) and in: Theoretical physics and astrophysics. p. 126 transl. D. Ter Haar. Oxford: Pergamon 1979. The energy of the photon is given by $\hbar\omega$, while its momentum in a medium of refractive index 'n' is given by $h/\lambda = \hbar\omega n$
3. J.D. Jackson: Classical electrodynamics. p. 498. New York: Wiley 1966; W.K.H. Panofsky, M. Phillips: Classical electricity and magnetism. p. 374. Reading: Addison-Wesley 1962
4. L.I. Schiff: Quantum mechanics 2nd edit. p. 270. New York: McGraw-Hill 1955
5. J.V. Jelley: Cerenkov radiation and its applications. London: p. 68. London: Pergamon 1958; J.D. Lawson: Philos. Mag. **45**, 748 (1954)
6. J. Litt, R. Meunier: Ann. Rev. Nucl. Sci. **23**, 1 (1973); R.S. Gilmore: Proceedings of the 1980 SLAC Summer Institute on Particles Physics SLAC-239 p. 265
7. J.G.H. de Groot et al.: Z. Phys. C - Particles and Fields **1**, 143 (1979); Phys. Lett. **82B** 292, 456 (1979); M. Holder, J. Steinberger: CERN rep. NP/JS/ih/125 (1974) (unpublished)
8. B.C. Barish et al.: Proceedings of the 9th SLAC Summer Institute of Particle Physics, Stanford 1981, E. Mosher ed. p. 641 (1982) (data of experiment E616 presented by P.A. Rapidis); R. Blair: A total cross section and y distribution measurement for muon type neutrinos and antineutrinos on iron. Ph.D. Thesis (1982) California Institute of Technology (unpublished)
9. D.A. Edwards, F.J. Sciulli: A second generation narrow band neutrino beam. Fermilab TM-660 (unpublished)
10. J. Lee: Measurements of neutrino charged current cross section from $E_\nu = 25$ GeV to 260 GeV. Ph.D. Thesis (1980) California Institute of Technology (unpublished) (experiment E356)
11. D.D. Yovanovitch et al.: Nucl. Instrum. Methods **94**, 477 (1971)
12. Note that classical optical diffraction sets an angular width to the focus of the Cerenkov light given by λ/D where D is the aperture of the principal mirror; this effect is negligible compared to all other sources of smearing
13. G.A. Cook ed.: Argon, Helium and the rare gases, p. 240. New York: Interscience 1961; A. Dalgarno, A.E. Kingston: Pro. Roy Soc. (London) **259A**, 424 (1961); E.R. Hayes et al.: Index and dispersion of some Cerenkov counter gases. ANL-6916 (1964) (unpublished), see also Litt and Meunier (Ref. 6) p. 10
14. V.L. Ginzburg, I.M. Frank: Ž. Èksperim Teoret. Fiz. **16**, 15 (1946)
15. E. Janikova et al.: Nucl. Instr. Meth. **74**, 61 (1969); V.Y. Pafomov: Izv. Yyss. Ucebn. Zaved. Radiofizika **5**, 484 (1962); Joint Publ. Res. Serv. 5 148 (1962)
16. V.P. Zrelov, J. Ruzicka: Nucl. Instrum. Methods **151**, 395 (1978)
17. P. Goldsmith, J.V. Jelley: Philos. Mag. **4** (1959)
18. J.V. Jelley (Ref. 5) p. 70 quotes a report by E.W.T. Richards: A.E.R.E. Report No. C/R 1901, Harwell, UK (1956)
19. S. Prunster et al.: Phys. Lett. **28B**, 47 (1968); J. Oostens et al.: Phys. Rev. Lett. **19**, 541 (1967); F. Inman, J.J. Murrey: Phys. Rev. **142**, 272 (1966)
20. L. Wartski: J. Appl. Phys. **46**, 3644 (1975)
21. V.P. Zrelov, J. Ruzicka: Nucl. Instrum. Methods **165**, 91 (1979)
22. F.R. Arutyunyan et al.: Sov. Phys. JETP (Engl. Transl.) **38**, 5 (1974) (Zh. Eksp. Teor. Fiz. **65**, 1772 (1973)